Calculation of the ionization rate and electron transport coefficients in an argon rf discharge

P. M. Meijer, W. J. Goedheer, and J. D. P. Passchier
FOM–Instituut voor Plasmafysica "Rijnhuizen," P.O. Box 1207, 3430 BE Nieuwegein, The Netherlands
(Received 26 July 1991)

The behavior of an rf discharge can be modeled by using a fluid approach. For this approach, the values of the mobility and diffusion coefficients as well as the ionization rate are necessary. These values are often obtained by extrapolating the data of dc Townsend discharges. To check whether this is justified we computed the coefficients for electrons in an rf discharge by using a kinetic model based on a two-term approximation of the electron energy distribution function. The calculated electron mobility and electron diffusion coefficients agree reasonably well with the extrapolated Townsend values. Significant deviations were found between the extrapolated Townsend ionization rate and the computed rf ionization rate as a function of the reduced electric field.

PACS number(s): 52.80.Pi, 51.50.+v, 52.25.Dg, 52.40.Hf

I. INTRODUCTION

Radio-frequency discharges are commonly used for the etching of thin films. High etch rates, good selectivities, and highly anisotropic etch profiles can be achieved by using rf plasma etching techniques. These characteristics favor rf plasma etching above wet etching methods.

In recent years, there has been a growing interest in modeling rf discharges. Several models have been developed to describe, e.g., the ion dynamics [1], the electron dynamics [2,3], and the sheath dynamics [4,5], of these discharges.

We will give particular attention to the fluid models for rf conditions [6–12]. These models describe the discharge self-consistently by solving the continuity, the momentum, and the energy equations for the electrons and the (positive and negative) ions coupled with the Poisson equation for the potential distribution in the discharge. The rf transport coefficients (mobility and diffusion) and the ionization rate are often extracted from data for Townsend discharges, see, e.g., Refs. [6–8].

These Townsend transport coefficients must be extrapolated toward rf discharge conditions. As the reduced rf electric field (typically $E/p=2$ kV $\mathrm{m}^{-1}\mathrm{Pa}^{-1}p$ represents pressure) [8] is almost a factor of 10 higher than the field in a Townsend discharge (typically $E/p=0.2\,\mathrm{kV\,m^{-1}\,Pa^{-1}}$) [13], it is, *a priori,* not clear whether these extrapolated Townsend data can be used for rf conditions.

In this paper, the ionization rate and the electron transport coefficients (mobility and diffusion) are computed as a function of the reduced electric field by using a kinetic model for the electrons of rf discharges, which is based on a two-term approximation of the electron energy distribution function. We calculated the electron transport coefficients and ionization rate and compared these coefficients with the extrapolated Townsend data.

II. THE TOWNSEND DATA

To illustrate that the extrapolation of the Townsend transport coefficients gives unrealistic results, the relation between the average electron energy $\langle eu \rangle$ (eV) and the reduced electric field E/p ($\mathrm{kV\,m^{-1}\,Pa^{-1}}$) as used by Richards, Thompson, and Sawin [7] is considered:

$$\langle eu \rangle = 5.3 + 43.9(E/p) , \tag{1}$$

where $-e$ is the electron charge. This relation is a reasonable estimate for the average electron energy in Townsend discharges, where $E/p \approx 0.2\ \mathrm{kV\,m^{-1}\,Pa^{-1}}$ [13]. However, it gives totally unrealistic energies when it is extrapolated toward rf conditions, viz. (1) yields $\langle eu \rangle \approx 93$ eV for a realistic rf field of $E/p \approx 2\ \mathrm{kV\,m^{-1}\,Pa^{-1}}$, while it is well known that $\langle eu \rangle \leq 10$ eV [9].

To obtain the ionization rate as a function of the reduced field, Richards, Thompson, and Sawin also fitted the Townsend data, i.e.,

$$k_{\mathrm{ion}} = 3.86\times 10^{-13}(E/p)\exp[-0.74/(E/p)^{0.5}] . \tag{2}$$

Again, this relation gives unrealistic high values for an rf discharge, viz. $k_{\mathrm{ion}} \approx 5\times 10^{-13}\ \mathrm{m^3\,s^{-1}}$, while the actual rf ionization rate is of the order of $10^{-14}\,\mathrm{m^3\,s^{-1}}$ [9].

The two formulas (1) and (2) are combined by Richards, Thompson, and Sawin to get an expression of the ionization rate in terms of the average electron energy, i.e.

$$k_{\mathrm{ion}} = 8.7\times 10^{-15}(\langle eu \rangle - 5.3) \times \exp\left[\frac{-4.9}{(\langle eu \rangle - 5.3)^{0.5}}\right] . \tag{3}$$

Relation (3), which is valid in the Townsend regime, is often used in the continuity equation of an rf fluid model [8]. It is thus assumed that the electron energy distribution function in the Townsend regime is similar to the distribution function in the rf regime. It should be noted that for an rf plasma, the average energy is not determined by relation (1) but is computed by solving the energy balance for electrons [7,8].

Not only the ionization rate, but also the electron mobility coefficient and the electron diffusion coefficient are extrapolated toward rf conditions.

III. THE KINETIC MODEL

A planar reactor is considered with an electrode separation $2L$ and an rf electric field $E(x,t)$ in the x direction only. The evolution of the electron energy distribution function (EEDF) is described by the kinetic equation

$$\frac{\partial F_e}{\partial t}+v_{\parallel}\frac{\partial F_e}{\partial x}-\frac{eE}{m}\frac{\partial F_e}{\partial v_{\parallel}}=\left[\frac{\delta F_e}{\delta t}\right]_{\text{coll}} . \tag{4}$$

Here m is the electron mass, and $v_{\parallel}$ denotes the component of the electron velocity in the direction of the electric field. To find the basic behavior of the electron dynamics, we will use the well-known Lorentz (two-term) approximation [14]

$$F_e(x,v_{\parallel},v_{\perp},t)=F(x,v,t)+\left[\frac{v_{\parallel}}{v}\right]F_1(x,v,t) , \tag{5}$$

where $v=\sqrt{v_{\parallel}^2+v_{\perp}^2}$ is the electron velocity, F and F_1 denote the isotropic and anisotropic part of the EEDF, respectively.

The Lorentz approximation is correct for sufficiently small values of the electric field. As the rf electric fields are rather strong, especially in the sheath regions, it is, *a priori,* not clear whether the Lorentz approximation can be used under rf conditions. However, Feoktistov *et al.* showed that the Lorentz approximation yields results which agree well, at least for the spatial distributions of the mean electron energy and the ionization coefficient, with both a Monte Carlo simulation and a "back-forward" approximation [15]. He further showed that the range of the applicability of the Lorentz approximation is larger than one would normally expect and that the Lorentz approximation can be used for rf discharge modeling.

Radio-frequency plasmas are weakly ionized. Therefore only electron–neutral-species collisions are taken into account. The inelastic electron–neutral-species collisions considered are electronic excitation and ionization. The description of these collisions is simplified by using an expansion of the collision integrals with respect to the ratio of the electron mass to the neutral-particle mass and truncating this expansion after the leading term [16]. Ionization results in an extra electron. It is assumed that the available energy is equally distributed amongst the two electrons.

By using (5) and by using the above approximations of the collision terms, the kinetic equation (4) is transferred into two coupled partial differential equations (PDE's) [14,17], viz,

$$\begin{aligned}\sqrt{mu/2e}\frac{\partial F}{\partial t}+\frac{1}{3}u\frac{\partial F_1}{\partial x}-\frac{E}{3}\frac{\partial(uF_1)}{\partial u}&=+4(2u+U_{\text{ion}})NQ_{\text{ion}}(2u+U_{\text{ion}})F(x,2u+U_{\text{ion}},t)\\&\quad+(u+U_{\text{exc}})NQ_{\text{exc}}(u+U_{\text{exc}})F(x,u+U_{\text{exc}},t)\\&\quad-uN[Q_{\text{ion}}(u)+Q_{\text{exc}}(u)]F(x,u,t),\end{aligned} \tag{6a}$$

$$\sqrt{m/2e}\frac{\partial F_1}{\partial t}+\sqrt{u}\left[\frac{\partial F}{\partial x}-E\frac{\partial F}{\partial u}\right]+\sqrt{u}NQ_m(u)F_1=0 . \tag{6b}$$

Here, $eu=mv^2/2$ denotes the electron energy in electron volts, $eU_{\text{ion}},eU_{\text{exc}}$ is the threshold energy for ionization and excitation, $Q_{\text{ion}},Q_{\text{ion}}(u)$ and $Q_{\text{exc}}=Q_{\text{exc}}(u)$ are the total cross section for ionization and excitation, respectively, $Q_m=Q_d+Q_{\text{ion}}+Q_{\text{exc}}$ is the total cross section for momentum dissipation, Q_d is the cross section for momentum scattering for elastic collisions, and N denotes the gas density.

The temporal behavior of F and F_1 is governed by the relation between the reduced collision frequencies for momentum and energy dissipation,

$$\frac{\nu_m}{N}=Q_m\sqrt{2eu/m} , \quad \frac{\nu_e}{N}=(Q_{\text{ion}}+Q_{\text{exc}})\sqrt{2eu/m} , \tag{7}$$

and the reduced rf angular field frequency ω/N [17]. In Fig. 1 these frequencies are plotted as a function of energy for a 13.6-MHz, 30-Pa ($N=7\times10^{21}$ m^{-3}) argon rf discharge. The cross sections are based on Refs. [18–21]. Because many scattering collisions occur in an rf cycle ($\nu_m/N\gg\omega/N$), the quasi-steady-state approximation can be used for (6b). Substitution of this solution into (6a) results in a second-order linear parabolic PDE for F, viz. [22],

$$\begin{aligned}&\sqrt{mu/2e}\frac{\partial F}{\partial t}-\frac{g}{3}\frac{\partial^2 F}{\partial x^2}-\frac{E^2}{3}\frac{\partial}{\partial u}\left[g\frac{\partial F}{\partial u}\right]+\frac{g}{3}\frac{\partial}{\partial x}\left[E\frac{\partial F}{\partial u}\right]+\frac{E}{3}\frac{\partial}{\partial u}\left[g\frac{\partial F}{\partial x}\right]\\&=4(2u+U_{\text{ion}})NQ_{\text{ion}}(2u+U_{\text{ion}})F(x,2u+U_{\text{ion}},t)+(u+U_{\text{exc}})NQ_{\text{exc}}(u+U_{\text{exc}})F(x,u+U_{\text{exc}},t)\\&\quad-uN[Q_{\text{ion}}(u)+Q_{\text{exc}}(u)]F(x,u,t) ,\end{aligned} \tag{8}$$

where $g=u/NQ_m$. Equation (8) is valid in the frequency regime $\omega\ll\nu_m$. The time derivative is included in (8) because, depending on electron energy, ν_e/N is greater or smaller than ω/N, see Fig. 1.

In order to solve (8) numerically, the distribution $F(x,u,t)$ is represented by discrete values on grid points in the x-u phase space. For each grid point the derivatives and source terms of (8) are approximated by finite

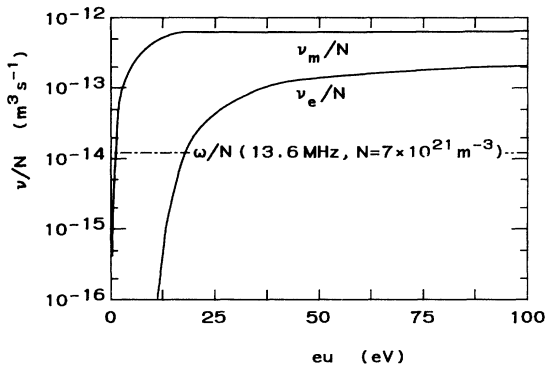

FIG. 1. The reduced frequency for momentum ν_m/N and energy ν_e/N dissipation as a function of electron energy for argon. Dashed line denotes the reduced angular rf frequency at 13.6 MHz for a pressure of 30 Pa ($N=7\times10^{21}$ m^{-3}).

differences. The electric field is approximated by a model field:

$$E(x_{\pm},t)=\frac{255}{L}\left[\frac{x}{L}\right]^5[1\pm\sin(\omega t)] . \tag{9}$$

Here, $x_{\pm}$ denotes $x\geq 0$ and $x<0$. The features of this field coincide with actual rf conditions, i.e., a high average electric field (≈ 25.5 kV m^{-1}) in the sheath region, a small electric field in the glow region, and a harmonic-oscillating behavior in time.

Starting from an initial condition $F(x,u,0)$, time integration is continued until periodicity is achieved. Time stepping is performed by using an implicit Euler method. Implicit methods are unconditionally stable; the time step can thus be taken as a fraction (e.g., 0.025) of the rf period. The implicit Euler method results in a linear system. This system is, for every time step, solved by a V-cycle multigrid iteration with one block u-line and one block x-line Gauss-Seidel iteration as a smoother [23]. A detailed description of the method of solution is given in Ref. [24].

In order to prevent the occurrence of the trivial solution, it is assumed that the EEDF is Maxwellian with an electron temperature of 4 eV at the electrodes. This boundary condition hardly influences the EEDF in the discharge.

Once the period solution F is known, the important macroscopic quantities such as electron density, electron flux, transport coefficients, etc., can easily be calculated as a function of time and position in the discharge. For instance, the electron density is given by

$$n(x,t)=4\pi\sqrt{2}\left[\frac{e}{m}\right]^{3/2}\int_0^{\infty}du\,F\sqrt{u} , \tag{10}$$

the ionization rate reads

$$Nnk_{\text{ion}}=8\pi\left[\frac{e}{m}\right]^2\int_{U_{\text{ion}}}^{\infty}du\,NuQ_{\text{ion}}F , \tag{11}$$

and the electron flux satisfies

$$\Gamma(x,t)=-\frac{\partial(Dn)}{\partial x}-\mu nE , \tag{12}$$

where D denotes the diffusion coefficient:

$$Dn=\frac{8\pi}{3}\left[\frac{e}{m}\right]^2\int_0^{\infty}du\,gF , \tag{13}$$

and μ is the mobility coefficient:

$$\mu n=-\frac{8\pi}{3}\left[\frac{e}{m}\right]^2\int_0^{\infty}du\,g\left[\frac{\partial F}{\partial u}\right] . \tag{14}$$

Usually, the spatial dependence of the electron density is much more pronounced that that of the diffusion coefficient. Consequently (12) can be written in the more familiar form

$$\Gamma(x,t)=-D\frac{\partial n}{\partial x}-\mu nE . \tag{15}$$

From this point we will only consider the periodic solution beginning at $\omega t=0$ and ending at $\omega t=2\pi$.

Equation (8) is linear in F and therefore its periodic solution is normalized with respect to the electron density in the center of the discharge ($x=0$) at time $\omega t=0$, i.e., F is rescaled such that $n(0,0)=1$.

IV. RESULTS

Results are shown for a 13.6-MHz argon ($eU_{\text{ion}}=15.8$ eV, $eU_{\text{exc}}=11.5$ eV) rf discharge, operating at a pressure of 30 Pa ($N=7\times10^{21}$ m^{-3}), with an electrode separation of 0.02 m ($L=0.01$ m).

In Fig. 2 the normalized electron density n and the corresponding ionization rate Nnk_{ion} are plotted as a function of position at $\omega t=0$. The figure clearly shows the inhomogeneous character of the electron dynamics. In accordance with the results of Barnes, Cotler, and Elta [9], the ionization peaks just in front of the plasma sheath edge.

In Fig. 3 the average electron energy is plotted as a function of the reduced field. The original data from Golant [13], which is fitted by Richards, Thompson, and Sawin [7], is denoted by open circles. The solid lines denote the results of the kinetic model. The calculations show that the average electron energy is not a unique function of the reduced field, but oscillates in time between the value at $\omega t=0$ and $\pi/2$. As mentioned earlier,

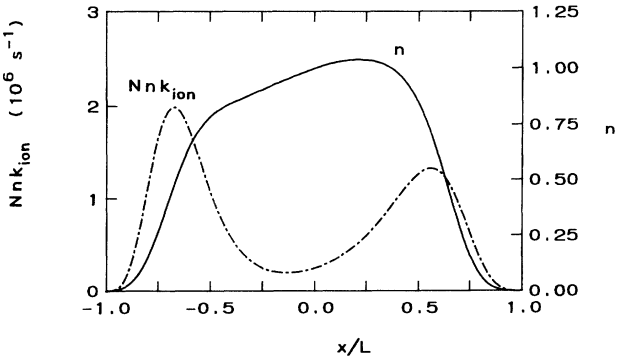

FIG. 2. The normalized electron density (solid line) and corresponding ionization rate per electron (dashed line) as a function of position at ($\omega t=0$) for 13.6 MHz.

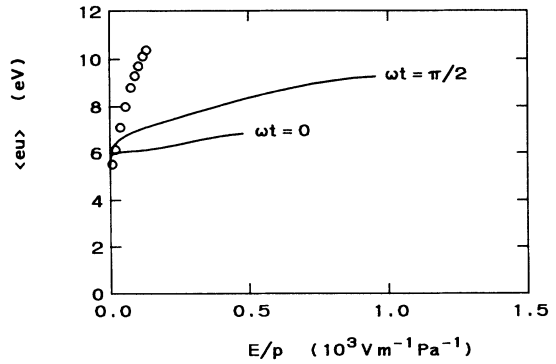

FIG. 3. The average electron energy as a function of the reduced field. The solid lines denote the solution of the kinetic model at two different times in the rf cycle and (○) denotes the data for a Townsend discharge.

the extrapolation of the Golant data yields unrealistic electron energies. The kinetic approach yields realistic average electron energies, viz., it varies between approximately 5 and 10 eV [9].

In Fig. 4 the ionization rate is plotted as a function of the average electron energy. The dotted curve is the result of the model of Barnes, Cotler, and Elta, the solid line is the kinetic model, the open circles denote expression (3). The figure shows that the kinetic model yields ionization rates which are somewhat smaller than the results of Barnes, Cotler, and Elta. This is probably caused by the neglect of the spatial diffusion in the model of Barnes, Cotler, and Elta. Note that the ionization rate calculated by using (3) agrees surprisingly well with the value of the kinetic model. Though (1) and (2) are both nonvalid for rf conditions, their combination results in a realistic prescription for the ionization rate. This seemingly surprising result is caused by the fact that Richards, Thompson, and Sawin used expressions which are correct for Townsend discharges, i.e., for discharges with $\langle eu \rangle$ between 5 and 10 eV. Since the average electron energy calculated with the kinetic rf model is in the same range, the rf ionization rate should not differ too much from the Townsend rate.

In Figs. 5(a) and 5(b) the mobility μ and diffusion D coefficient as calculated by using the kinetic model are

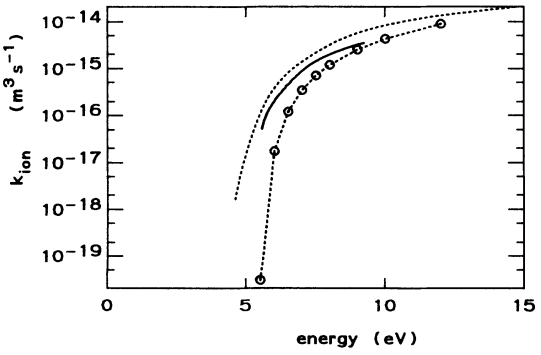

FIG. 4. The ionization rate as a function of the average electron energy. The dotted line denotes the solution of Barnes, Cotler, and Elta,the solid line is the kinetic model, and (○) denotes relation (3).

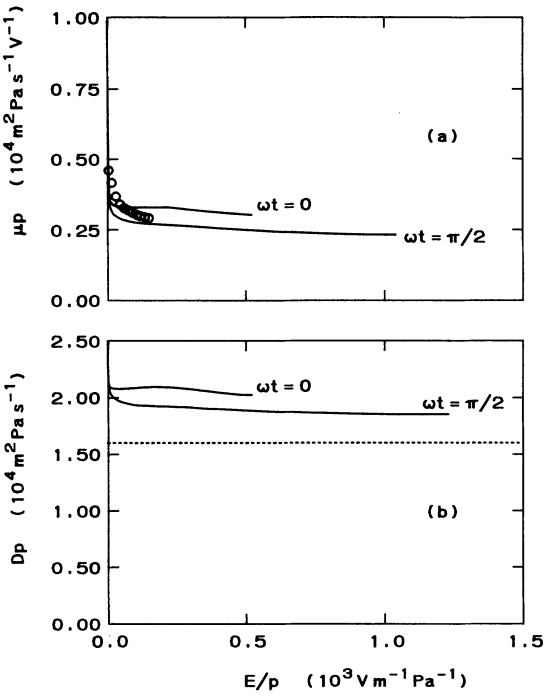

FIG. 5. The electron mobility (a) and the diffusion coefficient (b) as a function of the reduced field. The solid lines represent the solution of the kinetic model at two different times in the rf cycle, (○) is the data of Golant [13], and the dashed line is the Townsend value used by Richards, Thompson, and Sawin [7].

plotted as a function of the reduced field, respectively. Also plotted are the mobility coefficient (indicated by open circles) in a Townsend discharge found by Golant [13], and the diffusion (dashed line) coefficient used by Richards, Thompson, and Sawin. The kinetic model yields a time-dependent mobility and diffusion coefficient. Both the diffusion and mobility are rather insensitive to the value of E/p and to the phase in the rf cycle for both Townsend as well as rf conditions. So, it is allowed to take them constant in the Townsend regime and to use this constant value in the rf regime as was done by Richards, Thompson, and Sawin [7] and Oh, Choi, and Choi [8]. Note the good agreement between the mobility coefficient obtained form the Golant data and the results of the kinetic model. The deviation between the calculated diffusion coefficient and the value used by Richards, Thompson, and Sawin is somewhat larger. This is probably due to different pressure in the discharge. Richards, Thompson, and Sawin derived their data from the calculation of Lowke and Davies [25] for a high-pressure (3.2×10^4 Pa) discharge. This pressure is much higher than the pressure of 30 Pa that is used in our calculations. The latter is a typical value for an rf discharge.

V. CONCLUSIONS

The electron transport coefficients and ionization rate are calculated for rf discharges by using a kinetic model. These calculations show that both the electron mobility and the electron diffusion coefficients can be taken form Townsend experiments without introducing serious errors. It is not allowed to extrapolate the Townsend rela-

tion between the average electron energy and the reduced electric field towards rf conditions. This also holds for the ionization rate as a function of the reduced field. Nevertheless, it has been shown that the direct relation between the ionization rate and the averaged electron energy, as valid for the Townsend regime, can also be used for rf discharges.

ACKNOWLEDGMENTS

This work was performed under the EURATOM-FOM Association agreement and was supported by The Netherlands Organization for Fundamental Research (NWO), the Netherlands Technology Foundation (STW), and EURATOM.

[1] W. J. Goedheer and P. M. Meijer, IEEE Trans. Plasma Sci. **PS-19**, 245 (1991).
[2] J. V. DiCarlo and M. J. Kushner, J. Appl. Phys. **66**, 5763 (1989).
[3] T. J. Sommerer, W. N. G. Hitchon, R. E. P. Harvey, and J. E. Lawler, Phys. Rev. A **43**, 4452 (1991).
[4] P. M. Meijer and W. J. Goedheer, Phys. Fluids B **3**, 1804 (1991).
[5] S. Biehler, Appl. Phys. Lett. **54**, 317 (1989).
[6] J. -P. Boeuf, Phys. Rev. A **36**, 2782 (1987).
[7] A. D. Richards, B. E. Thompson, and H. H. Sawin, Appl. Phys. Lett. **50**, 492 (1987).
[8] Yank-oH Oh, Nak-Heon Choi, and Duk-In Choi, J. Appl. Phys. **67**, 3264 (1990).
[9] M. S. Barnes, T. J. Cotler, and M. E. Elta, J. Comput. Phys. **77**, 53 (1988).
[10] D. B. Graves and K. F. Jensen, IEEE Trans. Plasma Sci. **PS-14**, 78 (1986).
[11] S.-K Park and D. J. Economou, J. Appl. Phys. **68**, 3904 (1990).
[12] V. V. Boiko, Yu. A. Mankelevich, A. T. Rakhimov, N. V. Suetin, V. A. Feoktistov, and S. S. Filippov, Fiz. Plazmy **15**, 218 (1989) [Sov. J. Plasma Phys. **15**, 126 (1989)].
[13] V. E. Golant, Zh. Tekh. Fiz. **29**, 756 (1959) [Sov. Phys. Tech. Phys. **4**, 680 (1959)].
[14] I. P. Shkarofsky, T. W. Johnston, and M. P. Bachyniski, *The Particle Kinetics of Plasmas* (Addison-Wesley, Reading, 1966), p. 77.
[15] V. A. Feoktistov, A. M. Popov, O. B. Popovicheva, A. T. Rakhimov, T. V. Rakhimova, and E. A. Volkova, IEEE Trans. Plasma Sci. **PS-19**, 163 (1991).
[16] J. Wilhelm and R. Winkler, Beitr. Plasmaphys. **7**, 333 (1979).
[17] R. Winkler and J. Wilhelm, Ann. Phys. (Leipzig) **42**, 537 (1985).
[18] F. J. de Heer, R. H. J. Jansen and W. van de Kaay, J. Phys. B **12**, 979 (1979).
[19] H. B. Milloy, R. W. Crompton, J. A. Rees, and A. G. Robertson, Aust. J. Phys. **30**, 61 (1977).
[20] K. L. Bell, N. S. Scott, and M. A. Lennon, J. Phys. B **17**, 4757 (1984).
[21] J. C. Nickel and K. Imre, in *Proceedings of the 13th International Conference on the Physics of Electronic and Atomic Collisions, Berlin, Germany, 1983,* edited by J. Eichler, W. Fritsch, I. V. Hertel, N. Stolterfoht, and U. Wille (International Conference on the Physics of Electronic and Atomic Collisions, Berlin, 1984), p. 93.
[22] N. L. Aleksandrov, A. V. Molchek, N. A. Dyatko, I. V. Kochetov, and A. P. Napartovich, Fiz. Plazmy **14**, 334 (1988) [Sov. J. Plasma Phys. **14**, 196 (1988)].
[23] W. Hackbusch, *Multi-Grid Methods and Applications* (Springer-Verlag, Berlin, 1985).
[24] P. M. Meijer, FOM–Instituut voor Plasmafysica "Rÿnhuizen" Report No. 91-203, 1991 (unpublished).
[25] J. J. Lowke and D. K. Davies, J. Appl. Phys. **48**, 4991 (1977).